PALEONTOLOGY

Decoupling biogeochemical records, extinction, and environmental change during the Cambrian SPICE event

James D. Schiffbauer,[1]* John Warren Huntley,[1] David A. Fike,[2] Matthew Jarrell Jeffrey,[1] Jay M. Gregg,[3] Kevin L. Shelton[1]

Several positive carbon isotope excursions in Lower Paleozoic rocks, including the prominent Upper Cambrian Steptoean Positive Carbon Isotope Excursion (SPICE), are thought to reflect intermittent perturbations in the hydrosphere-biosphere system. Models explaining these secular changes are abundant, but the synchronicity and regional variation of the isotope signals are not well understood. Examination of cores across a paleodepth gradient in the Upper Cambrian central Missouri intrashelf basin (United States) reveals a time-transgressive, facies-dependent nature of the SPICE. Although the SPICE event may be a global signal, the manner in which it is recorded in rocks should and does vary as a function of facies and carbonate platform geometry. We call for a paradigm shift to better constrain facies, stratigraphic, and biostratigraphic architecture and to apply these observations to the variability in magnitude, stratigraphic extent, and timing of the SPICE signal, as well as other biogeochemical perturbations, to elucidate the complex processes driving the ocean-carbonate system.

INTRODUCTION

The Early Paleozoic era [~541 to 444 million years ago (Ma)] encompasses an important time frame in metazoan evolution, including the Cambrian Explosion and the Great Ordovician Biodiversification Event. This interval is marked by recurrent extinction and recovery events, and the highest origination rates in the Phanerozoic (1, 2). In addition, biogeochemical data from the early Paleozoic indicate intermittent perturbations in the carbon sedimentary isotopic records [for example, see the studies by Gill *et al.* (3), Jones and Fike (4), and Saltzman *et al.* (5)], with several prominent positive carbon isotopic excursions (positive shifts in $\delta^{13}C$, or increased $^{13}C/^{12}C$ ratios) that are attributed to a variety of secular changes in global ocean chemistry (6). The Upper Cambrian Steptoean Positive Carbon Isotope Excursion (SPICE) has been proposed as a globally synchronous event that was initiated at the *Crepicephalus-Aphelaspis* biozone boundary and biotic crisis (Marjumiid-Pterocephaliid biomere boundary) (7). The SPICE event is thought to have been contemporaneous with the following: (i) a radiation of phytoplankton, zooplankton, and suspension feeders, as well as a consequent increase in ecological complexity (8), and (ii) an increase in atmospheric oxygen (9), possibly associated with an oceanic anoxic/euxinic event (3). Conceptual models have been constructed to explain the causes and effects of these sundry secular changes, including ocean anoxia/euxinia driving trilobite turnover, associated enhancement of organic carbon and pyrite burial forcing changes in atmospheric oxygen levels, and oxygenated coastal waters driving the diversification of plankton and perhaps the resulting Ordovician biodiversification (3, 9, 10). However, the geographic and temporal synchronicity; the correspondence in time with trilobite biotic turnover; the varying degrees of alteration by diagenetic processes; the regional variation in shape, magnitude, and stratigraphic thickness; and the facies dependence of the SPICE event remain largely unresolved. The need to address these types of questions has been highlighted by recent work demonstrating depositional and diage-

netic controls on $\delta^{13}C$ variation during positive excursions [for example, see the study by Metzger and Fike (11)] as well as $\delta^{13}C$ analyses of geologically recent carbonate banks (12), suggesting that these isotopic excursions can be more directly linked to local, rather than global, processes. Representing a depth gradient from basinal to lagoonal paleoenvironments with ample off-shore fossil control, the Upper Cambrian strata of southeastern Missouri are ideal for testing the competing effects of global ocean chemistry versus local carbon productivity and burial on carbon isotopic signatures, and the relationship of these signatures to biotic turnover and facies architecture.

Geological and paleontological setting

The carbonate-dominated Sauk megasequence of the Late Cambrian central Missouri intrashelf basin records variations in community paleoecology and both the depositional facies and inferred water depths (basin, basin margin, platform edge, and lagoonal back reef) (13, 14). To investigate regional variation of the SPICE, we examined rocks of the Bonneterre and Davis formations, which cross the Marjuman-Steptoean stage boundary and encompass major biotic and environmental perturbations—the Marjumiid-Pterocephaliid biomere turnover (Fig. 1) and marked changes in sea level (Sauk II regression–Sauk III transgression). This biomere boundary documents the latter phase of a two-phase extinction event, defined first by the extinction of most shallow marine trilobites (the *Crepicephalus* zone fauna) and second by the subsequent encroachment of a deeper-water trilobite fauna (the *Aphelaspis* zone fauna) onto the shallower shelf after an extinction of the *Crepicephalus* zone holdovers (the *Coosella perplexa* subzone fauna) (15–18). The duration between these two phases is denoted as a critical interval (15, 17) and has been thought previously to correspond to mechanisms such as the shallowing of the thermocline (19) and/or ecological turnover induced by sea-level rise (20, 21).

The SPICE was recognized previously near the western edge of the basin (3) and is present in shallow-water lithofacies proximal to the St. Francois Mountains (Fig. 1) (22). Here, we target drill cores along a paleodepth gradient for litho-, bio-, and chemostratigraphic analyses. The Cambrian strata of the Sauk megasequence of southeastern Missouri comprise small- to large-scale, unconformity-bounded,

[1]Department of Geological Sciences, University of Missouri, Columbia, MO 65211, USA. [2]Department of Earth and Planetary Sciences, Washington University in St. Louis, St. Louis, MO 63130, USA. [3]Boone Pickens School of Geology, Oklahoma State University, Stillwater, OK 74078, USA.
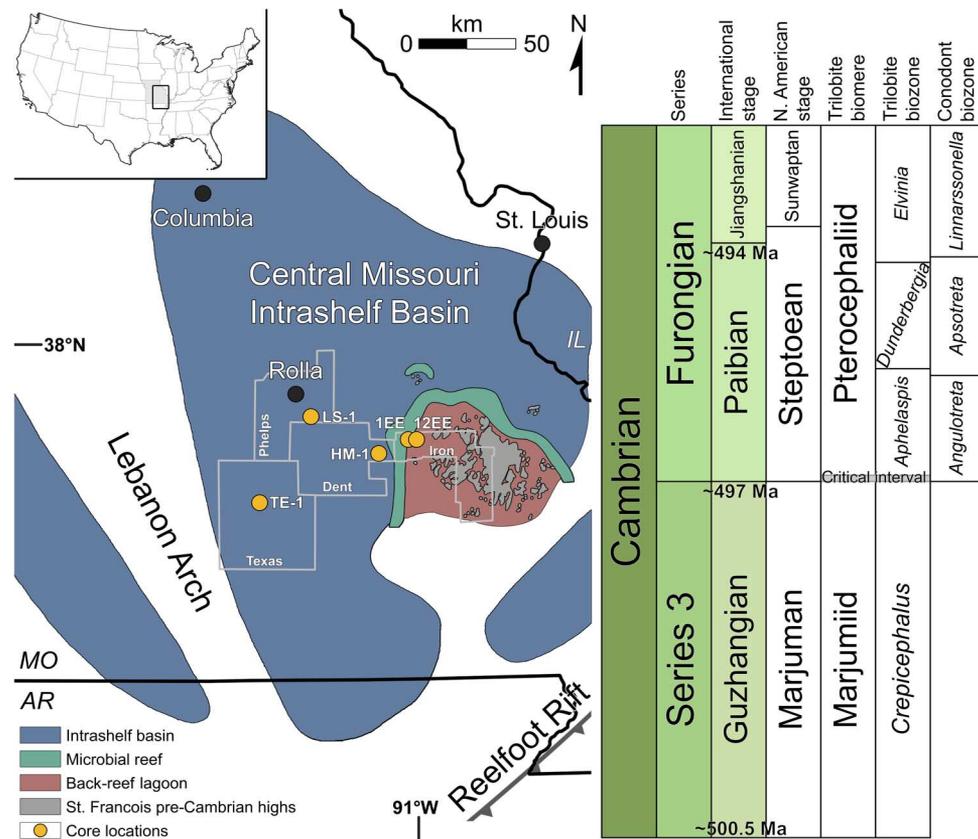*Corresponding author. Email: schiffbauerj@missouri.edu

Fig. 1. Drill core locality map (13, 24, 40, 41) with generalized Late Cambrian international and Laurentian chronostratigraphy, and trilobite and conodont biozonation (14, 18, 23, 43–46).

transgressive-regressive sequences, which are characterized by linear facies belts. Within this region, shale and micritic limestone of the intrashelf basin facies developed distal from basement highs, microbial bioherms and ooid grainstone of the platform edge facies formed narrow belts adjacent to highs, and microbial laminates and lagoonal mudstone "back reef–type" facies developed proximal to and within igneous islands (the modern St. Francois Mountains; Fig. 1). The Bonneterre Dolomite contains the Marjuman-Steptoean stage boundary, which corresponds to the critical interval of the *Crepicephalus-Aphelaspis* biotic turnover (Fig. 1). This stage boundary occurs typically within the upper two units of the Bonneterre: the Whetstone Creek and Sullivan Siltstone members (also denoted as the Bonneterre-Davis transition zone). The contact with the overlying Davis Formation corresponds generally to the Sauk II–Sauk III regression, a major Laurentian fall in sea level, broadly equivalent to the uppermost *Dunderbergia*–lowermost *Elvinia* trilobite zones of the Steptoean stage. The Davis Formation, a mixed carbonate-clastic unit characterized by interbedded carbonates and shales of the intrashelf basin, encompasses the entirety of the Sauk III transgression through the beginning of the Hellnmaria Highstand (13).

RESULTS

The SPICE is expressed in our cores as ≤6‰ positive shift in the isotopic composition of carbonate carbon [$\delta^{13}C_{carb}$; reported in per mil Vienna Pee Dee Belemnite (‰ V-PDB)]. The onset and rising limb of the excursion are found in the upper Bonneterre, the Bonneterre-Davis transition zone (where noted), and the lower Davis formations (Fig. 2, figs. S1 to S5, and tables S1 to S5), coincident with the onset of the Sauk III transgression. The maximum value and subsequent $\delta^{13}C_{carb}$ decline in most drill cores are within the lower Davis, with the notable exception of the deepest-water core, LS-1, in which the excursion maximum occurs coincidently with the Bonneterre-Davis boundary. The immediately preceding baseline and SPICE maximum $\delta^{13}C_{carb}$ values covary with the inferred water depth. The deeper-water cores, LS-1 and HM-1, show maxima of ~4.2 and ~5.7‰, respectively, both with the preexcursion baseline values near 0‰. The shallower-water cores, 1EE and 12EE, exhibit lower maxima (~3.0 and ~2.4‰, respectively), and both have preexcursion baseline values <0‰. The previously published (3) basin margin core (TE-1) displays a maximum of ~3.8‰ (our new data maximum is ~2.6‰) and a preexcursion baseline again near 0‰. In TE-1, the rising limb, peak, and initial decline of the excursion all occur within the uppermost Bonneterre, whereas the excursion straddles the Bonneterre-Davis boundary in all other cores.

In TE-1, the onset of the SPICE is abrupt, initiating ~0.3 m above the base of a ~3-m-thick shale interval. The maximum $\delta^{13}C_{carb}$ value occurs 2.4 m above its onset, within the same shale interval. The descending limb of the SPICE displays a more gradual return to baseline $\delta^{13}C_{carb}$ values in silty carbonate rocks over a vertical distance of ~28 m. In LS-1, the SPICE begins in a dolomitic siltstone, reaches its maximum
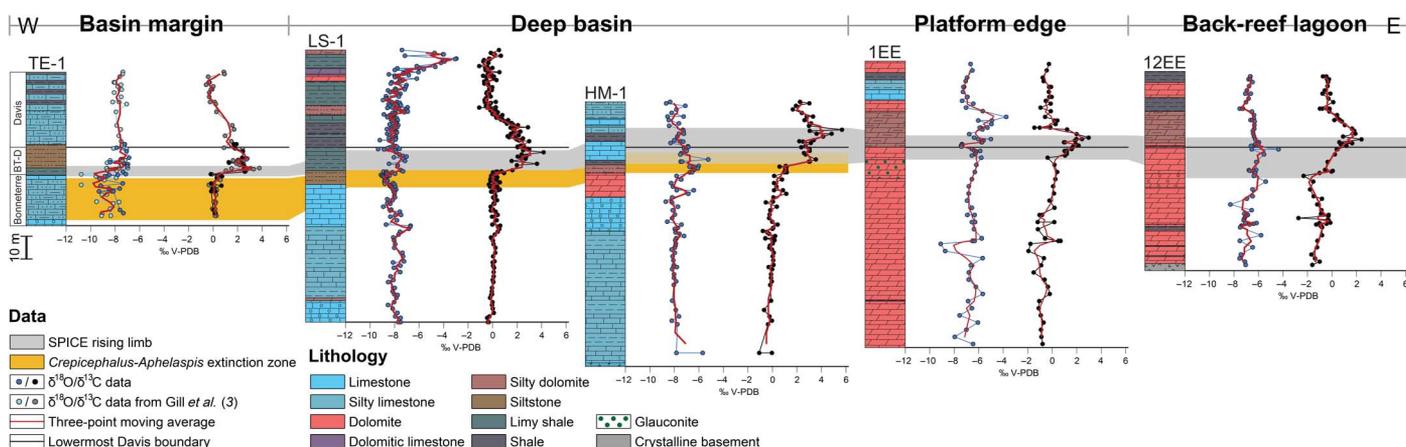
Fig. 2. Litho-, chemo-, and biostratigraphy of Upper Cambrian cores across the central Missouri intrashelf basin. The core data are plotted, from left to right, across a west-to-east trending transect, which represents a paleodepth gradient from the shallow basin margin along the Lebanon Arch (TE-1), to deep intrashelf basin (LS-1 and HM-1), to shallow platform edge (1EE) and back-reef lagoon (12EE) paleoenvironments. Gill *et al.* (*3*) values for TE-1 (light blue, $\delta^{18}O_{carb}$; gray, $\delta^{13}C_{carb}$) shown with corrected biostratigraphic placement (see also fig. S6). Blue circles, $\delta^{18}O_{carb}$ (‰ V-PDB) values; black circles, $\delta^{13}C_{carb}$ (‰ V-PDB) values. BT-D, Bonneterre-Davis transition zone.

8.5 m up-section within interbedded shale and limestone, and returns to baseline values 16.3 m above, in another dolomitic siltstone. HM-1 records a comparable scenario. In the platform edge core 1EE, the complete SPICE interval is expressed over the shortest vertical thickness, with the SPICE initiating in a recrystallized brown dolomite and the maximum $\delta^{13}C_{carb}$ value occurring 8.5 m above, in dolomite beds with minor shale. The upper limb of the SPICE returns to lower background values ~4.3 m above, in the same lithology. In the back-reef facies of the 12EE core, oolitic dolomite records the onset of the SPICE, which peaks ~15.5 m up-section within interbedded shale and subordinate dolomite, and returns ~13.1 m above the maximum in thin dolomite interbedded with shale.

DISCUSSION

In an effort to use the SPICE as a chronostratigraphic marker, previous reports [for example, studies by Gill *et al.* (*3*), Saltzman *et al.* (*7*), and Peng *et al.* *23*)] have placed the onset of SPICE at the Marjumiid-Pterocephaliid biomere boundary, which itself could be diachronous (*16*); however, our data demonstrate that the placement of the SPICE interval within a biostratigraphic framework is variable along the depth gradient (*14*, *24*). In LS-1, the rising limb of the SPICE begins at the *Crepicephalus-Aphelaspis* zone boundary and peaks within the *Elvinia* zone. In HM-1, the SPICE begins below the first occurrence of *Aphelaspis* and peaks at least as high (stratigraphically) as the *Elvinia* zone. Gill *et al.* (*3*) presented inconsistent data on the timing of the SPICE in TE-1, which prompted us to analyze additional, microdrilled samples. Specifically, Gill *et al.* (*3*) had placed the maximum of the excursion coincident with the *Crepicephalus-Aphelaspis* boundary (their Fig. 2 and fig. S5), although the reported raw data (their table S3) suggest instead that the excursion maximum is coincident with the *Aphelaspis-Dunderbergia* boundary (see fig. S6). New data corroborate the general pattern and magnitude of the SPICE $\delta^{13}C_{carb}$ signal reported by Gill *et al.* (*3*); however, reevaluation of biostratigraphy indicates that the proper placement of the onset of the SPICE interval is stratigraphically above the *Crepicephalus-Aphelaspis* transition. In TE-1, the SPICE peaks within the *Aphelaspis* zone and below the first

appearance datum of *Apsotreta attenuata*, which is broadly correlative with the *Dunderbergia* zone (fig. S6) (*24*). Thus, the SPICE interval appears to be more stratigraphically protracted in the deeper-water part of the intrashelf basin, spanning portions of up to four trilobite biozones that occupy no more than ±3 million years relative to the Series 3–Furongian boundary (~497 Ma), than in the shallower-basin margin (Fig. 2), although shallower sections could be more subject to stratigraphic condensation. The lack of blue water trilobites—and thus biostratigraphic control—further complicates attempts to constrain the timing of the SPICE along the full breadth of the depth gradient in the shallow-water cores (1EE and 12EE). However, the Bonneterre-Davis boundary, though likely time-transgressive, is well defined in these shallow-water cores. Lithologic change to finer-grained sediments and more siliciclastic input directly associated with this formation boundary, likely representing the onset of the Sauk III transgression, permit us to use the Bonneterre-Davis boundary as an appropriate first-order datum to correlate shallow- and deep-water cores. In both of these shallow-water cores, the onset of the SPICE occurs several meters below the Bonneterre-Davis boundary and peaks several meters above (Fig. 2 and figs. S4 and S5).

The variation of the stratigraphic thickness of the rising limb of the SPICE along a depth gradient shows a similar pattern to that of the magnitude of the $\delta^{13}C_{carb}$ excursion. The deepest-water core (HM-1) and intrashelf basin–to–platform edge drill cores (LS-1 and 1EE) record the rise of the SPICE over greater stratigraphic thicknesses (~16, ~8, and ~8 m, respectively) compared to that of the intrashelf margin drill core (TE-1; thickness, ~3 m). An exception to this pattern is seen in the back-reef (lagoonal) core (12EE), with the SPICE rise recorded over a stratigraphic thickness approaching that of the deepest-water core (Fig. 3). This should not be surprising because the lagoon was a highly efficient carbonate factory, keeping pace with the Sauk III sea-level rise with minimal interruption of sediment deposition. We suggest that more ^{13}C-depleted samples (with a minimum $\delta^{13}C_{carb}$ value preceding the onset of the SPICE of −2.32‰) from the shallow-water back-reef (lagoonal) paleoenvironments reflect enhanced C_{org} reoxidation in areas of partially restricted circulation. The maximum $\delta^{13}C_{carb}$ value at the peak of the SPICE (2.40‰) in the back-reef

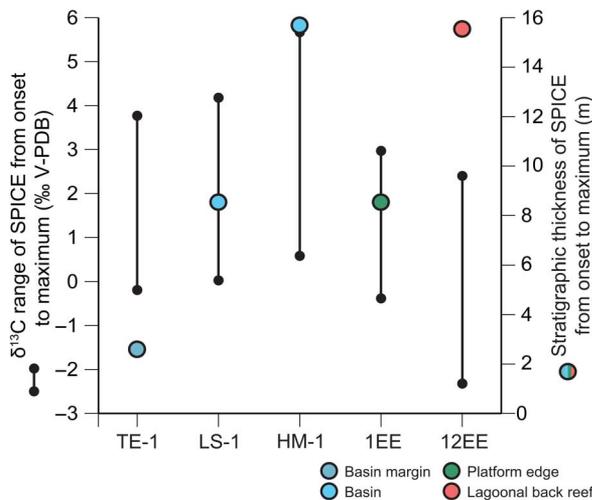**Fig. 3. Ranges of $\delta^{13}C_{carb}$ values from SPICE onset to maximum (SPICE rising limb; left y axis) and the corresponding stratigraphic thickness over which the rising limb of the SPICE is expressed (right y axis).**

environment is muted compared to deeper-water cores (>4‰), which likely records the integrated effect of the impinging ^{13}C-enriched water mass on the local $\delta^{13}C_{carb}$ reservoir (Fig. 4). The differential stratigraphic thickness of the SPICE represented here, across a regional depth gradient in the central Missouri intrashelf basin, highlights the necessity to reconsider the meaning of the variability of isotopic and stratigraphic records in other locations (for example, Smithfield Canyon, Utah; central Iowa; Port au Port, Newfoundland; and Nolichucky Formation, southwestern Virginia and northeastern Tennessee) (25, 26).

Similar lateral variability in $\delta^{13}C_{carb}$ exists in the geologic record (27–29), albeit from a number of possible causes such as water composition, sediment transport and terrestrial weathering, diagenesis, and primary productivity. For instance, higher $\delta^{13}C_{carb}$ values in deeper-water and lower $\delta^{13}C_{carb}$ values in shallow-water paleoenvironmental settings have been observed in settings such as the Pennsylvanian Paradox Basin (30), attributed to diachroneity in the deposition of parasequences with increased basin restriction distally. A comparable pattern has been found in modern carbonate settings (12, 31), such as south Florida and the Bahama Banks, attributed to terrestrial organic matter input from freshwater discharge (31). However, Cambrian terrestrial settings would have contributed very little, if any, organic matter; thus, modern carbonate settings (or even those in the Pennsylvanian) are unlikely to be appropriate or direct analogs for those existing before the evolution of land plants.

A simple pattern emerges from the lithologic context of the SPICE: the excursion is initiated at the onset of fine-grained sediment deposition during the Sauk III transgression (Fig. 2). In cores from the basin margin and deeper water, the SPICE is recorded largely within shale-limestone successions, bounded by carbonate-dominant lithologies of the underlying Bonneterre Formation and overlying upper Davis Formation. The shallower-water sections are more dolomitized than the deeper-water cores, and the magnitude of the SPICE in the former is muted compared to the latter. However, the carbon isotopic signals preserved in dolomite follow the same stratigraphic pattern as that observed in the limestone-dominant sections to the southwest, and the baseline $\delta^{13}C_{carb}$ values are broadly similar, suggesting that later dolomitizing fluids did not affect the $\delta^{13}C_{carb}$ signature, a reason-

able assumption such that $\delta^{13}C$ is typically more conservative than $\delta^{18}O$ in its response to dolomite recrystallization.

Our data show that the SPICE event in southeastern Missouri is a time-transgressive and facies-dependent phenomenon that is decoupled from the potentially diachronous Marjumiid-Pterocephaliid biotic crisis. Data from other worldwide localities are also consistent with this observation; the onset of the SPICE occurring before (for example, Kyrshabakty River, Kazakhstan; Wa'ergang and Paibi, Hunan, China; and Mt. Whelan, Queensland, Australia) (7, 32, 33), roughly coincident with (for example, Smithfield Canyon, Utah, and Shingle Pass, Nevada) (7, 25), and later than (Lawsons Cove, Utah; TE-1, Missouri; Nolichucky Formation, Virginia and Tennessee) (3, 26) the extinction horizon affirms diachroneity in these events. Facies and lithologic dependence of the SPICE signal is expressed by covariance of rock type and relative stratigraphic thickness over which the SPICE interval is recorded. In shale-dominated intervals, the rising limb of the SPICE signal, from onset to maximum, is stratigraphically abrupt (~3 m; for example, TE-1) (3). In contrast, thicknesses increase markedly in mixed carbonate-siliciclastic intervals (~15 to 100 m) (Smithfield Canyon, Utah; central Iowa; and Nolichucky Formation in Virginia and Tennessee) (25, 26) and more so in carbonate-dominated units (≥100 m; for example, Shingle Pass in Nevada and Mt. Whelan in Queensland, Australia) (3, 7). The recently described (26) $\delta^{13}C_{carb}$ trend in the mixed carbonate-siliciclastic Nolichucky Formation of the Appalachians, interpreted with a high rate of sediment accumulation, captures only the rising limb of the SPICE (and perhaps not completely) over tens of meters, but sampling density muddles the placement of its onset [for example, see the study by Myrow and Grotzinger (34)].

Although the SPICE is commonly represented as a geochemical record of the best-characterized oceanic anoxic event in the Paleozoic era (3), its facies dependence and variable stratigraphic occurrence relative to faunal transitions call into question its role as a driver of extinction (7, 16). However, other geochemical perturbations could be related to the biotic crisis. For instance, there appears to be an increased fluctuation of $\delta^{18}O_{carb}$ values (both positive and negative, preserved in both limestone and dolomite) across the extinction and near the onset of the SPICE in the two deep-water cores (LS-1 and HM-1), the basin margin core (TE-1), and the platform edge core (1EE), although it is less apparent in the back-reef core (12EE) (Fig. 2 and figs. S1 to S5). A similar shift in $\delta^{18}O_{carb}$, before and extending through the Marjumiid-Pterocephaliid biomere boundary, is observed in a shorter contemporaneous section, the Deadwood Formation, Black Hills, South Dakota (fig. S7), with meter-scale biostratigraphic control across the Crepicephalus-Aphelaspis boundary and varying chemostratigraphic sampling density. The vertical lithofacies sequence recorded in the lower Deadwood Formation corresponds to sea-level rise, representative of the Sauk II–Sauk III interval, during which cold water presumably impinged upon shallow-water continental shelves, permitting invasive opportunism of cold-water Aphelaspis trilobites (35, 36). The Marjumiid-Pterocephaliid biotic turnover recorded in this locality is temporally decoupled from the SPICE event. No positive carbon isotope excursion is recorded in this section (35); instead, a minor negative $\delta^{13}C_{carb}$ digression from baseline is coincident with the biotic turnover, similar in magnitude to that observed in the TE-1 core (fig. S6). The $\delta^{18}O_{carb}$ fluctuations in South Dakota and Missouri, although undoubtedly tenuous, occur at similar positions with respect to the Marjumiid-Pterocephaliid biotic crisis and are each discordant to the SPICE event, which itself supervenes these other geochemical and biotic markers.
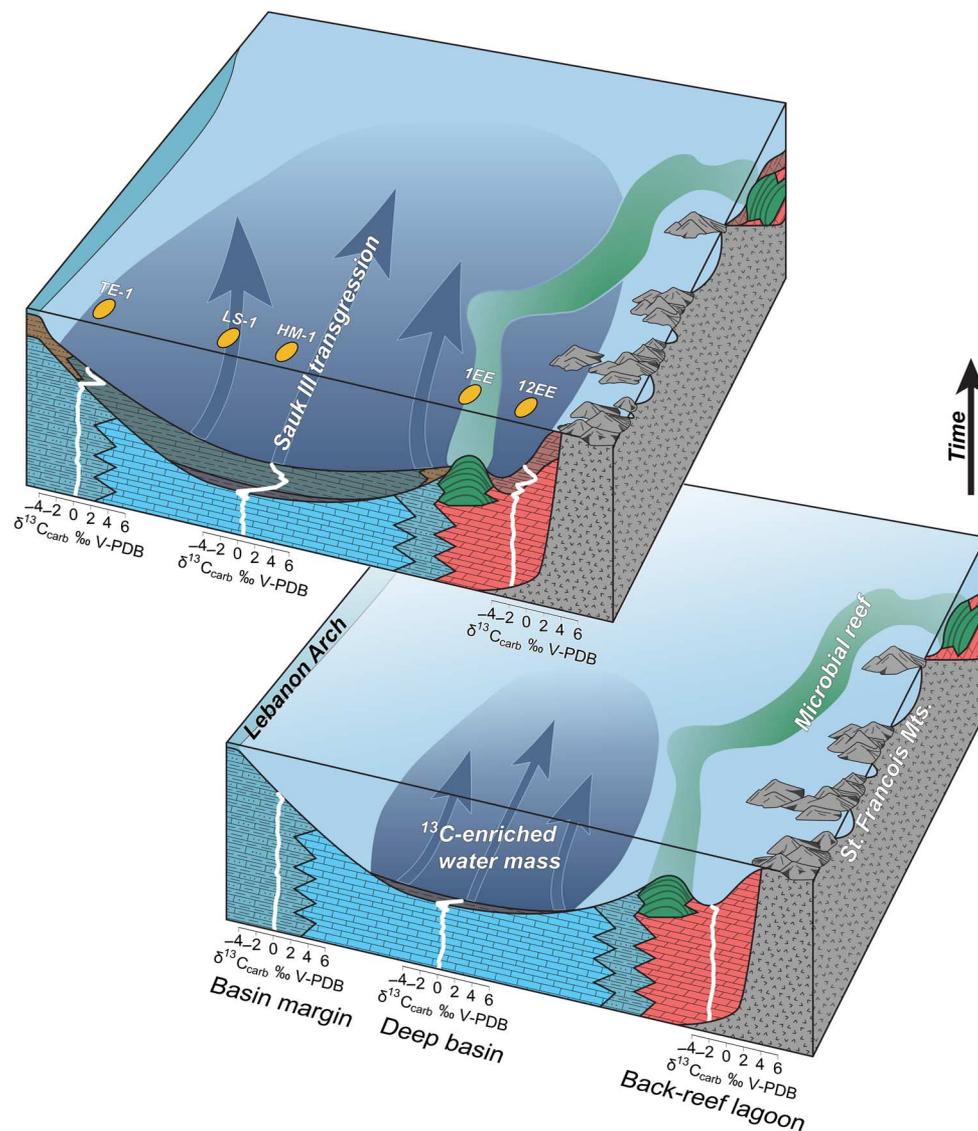
Fig. 4. Eustato-facies model illustrating the role of transgression and the impingement of ^{13}C-enriched water mass in recording the SPICE in the Upper Cambrian central Missouri intrashelf basin. Generalized core locations are shown in the upper panel, with the evolution of hypothetical $\delta^{13}C_{carb}$ curves shown corresponding to paleoenvironment and lithological changes.

In addition to the $\delta^{13}C_{carb}$ and $\delta^{18}O_{carb}$ biogeochemical records, $\delta^{34}S$ has been investigated as a proxy of sulfur cycling in seven localities that contain the SPICE interval (3, 37, 38). Most localities show parallel increases in sulfate ($\delta^{34}S_{CAS}$) and pyrite ($\delta^{34}S_{pyr}$) values, which are largely synchronous with the $\delta^{13}C_{carb}$ excursion. However, substantial variability is observed among the $\delta^{34}S$ records. The magnitude of the SPICE $\delta^{34}S_{CAS}$ excursion varies from 0‰ [Port Au Port Formation (37)] to ~10 to 15‰ [Shingle Pass, Lawson's Cove, and TE-1 (3, 38)] to ~30‰ [Mount Whelan-1 and Mount Murray (3)]. Similarly, the magnitude of the SPICE $\delta^{34}S_{pyr}$ excursion varies from ~0‰ [Port Au Port Formation (37)] to ~25‰ [Alum Shale (3)] to ~60‰ [Mount Whelan-1 and TE-1 (3)]. Given the variability in the magnitude and relative timing of the $\delta^{34}S$ excursions that broadly accompany the SPICE event, it appears that although an oceanic signature may be preserved, there are local geochemical signatures—potentially acquired

during deposition, early diagenesis, or late-stage alteration—that markedly and variably overprint any global signature. This geochemical variation has been recorded as locally smaller [for example, Port Au Port Formation (37)] or larger [for example, Mount Whelan-1 or Mount Murray (3)] magnitudes of excursions in the sulfur isotope records, consistent with our observations of local, facies-dependent control on the $\delta^{13}C_{carb}$ record and, more broadly, of the record of biogeochemical cycling [for example, see the studies by Gill *et al.* (38) and Kendall *et al.* (39)].

CONCLUSIONS

We interpret the variation of the $\delta^{13}C_{carb}$ signal across the depth gradient in southeastern Missouri to reflect the impingement of a deeper-water, more ^{13}C-enriched component on the local carbonate factory of the shallow-shelf environment, associated with the Sauk III transgression

(Fig. 4). Rather than regarding the SPICE event as the cause of biotic perturbation, it is better viewed as the integrated result of more complicated processes, perhaps including stratified ocean transgression and turnover [as indicated by Gill *et al.* (*3*)], which themselves may have affected the biota. On the basis of the available isotopic records through the Series 3–Furongian transition, we posit that there is commonality in carbonate depositional environments, broadly at lower latitudes, in which deeper, ^{13}C-enriched water invades carbonate platforms during the Sauk III transgression. Most interpretations of the SPICE implicate globally synchronous encroachment of deep anoxic or euxinic waters (*3*, *5*, *7*, *9*) in yielding the in-phase positive shifts in $\delta^{13}C_{carb}$ and $\delta^{34}S_{CAS}$. However, if the SPICE event reflects local facies change and differential recording of water masses, then it does not need to correspond directly to either global ocean anoxia or enhanced global carbon burial.

If the carbon isotope signals are the result of transgression of deeper waters onto carbonate platforms, the architecture of an individual platform will control where the invading water mass impinges and where within the stratigraphy it is recorded. Although the SPICE may represent a global signal, the manner in which it is recorded in rocks should vary as a consequence of bathymetry, platform geometry, local biological productivity, and water chemistry, which may collectively affect the magnitude, stratigraphic extent, and timing of the signal relative to (local) biotic events. Fundamentally, $\delta^{13}C$ data are used as a proxy to reconstruct carbon cycling, and the SPICE itself is only a signal, one in which any perturbations to the global carbon cycle are filtered through local depositional conditions. We need to shift the focus toward understanding the larger, more likely complicated processes (ocean chemistry, biotic turnover, and transgression, among others) that are driving the ocean carbonate system. Ultimately, we need better constraints on facies, stratigraphic, and biostratigraphic architecture to deconvolve the complexity of such a system.

MATERIALS AND METHODS

Appropriate cores, for which detailed logs exist (*24*) or for which descriptions were amended (*40*, *41*), were accessed from the Missouri Geological Survey McCracken Core Library and Research Center, including (from southwest to northeast) LS-1 (intrashelf basin), HM-1 (deepest-water intrashelf basin), 1EE (platform edge), and 12EE (back reef). In addition, the previously examined westernmost Texas County core (TE-1; intrashelf basin margin) (*3*) was resampled for completeness. Samples from each core were sectioned and examined by reflected light microscopy. Individual carbonate components (micritic calcite, ooids, and micritic dolomite) were microdrilled for carbon and oxygen isotope ratio mass spectrometry (IRMS) analysis, performed on GasBench II coupled to a Delta V Advantage IRMS at Washington University in St. Louis and a Kiel III device coupled to a Thermo Finnigan Delta-Plus IRMS at the University of Missouri. All isotopic data ($n = 455$) are reported as per mil deviation from V-PDB, with SEs of <±0.05‰ based on replicate analyses of NBS 19 limestone.

Typically, dolomites have been avoided in previous studies because of the possibility of isotopic exchange with late diagenetic/hydrothermal fluids. We specifically microsampled fine-crystalline, planar, and non–fabric-destructive (*42*) replacement dolomite to avoid these concerns, and the carbon isotopic signals observed here follow the same stratigraphic pattern as observed in the limestone-dominant sections to the southwest.

Biostratigraphic control for cores TE-1, LS-1, and HM-1 is from Kurtz *et al.* (*24*). Although biozones are defined by first appearance data,

we should note the caveat that fossil sampling is inherently more restricted with core samples relative to outcrop surveys; therefore, an increased and unavoidable uncertainty of fossil occurrences exists. For this reason, we have indicated a zone of uncertainty for the placement of the *Crepicephalus-Aphelaspis* biozone boundary bracketed between the last occurrence of *Crepicephalus* or *Tricrepicephalus* and the first occurrence of *Aphelaspis* or the broadly coincident conodont *Angulotreta*. Therefore, the *Crepicephalus-Aphelaspis* extinction zone referenced in Fig. 2 should not be confused with the so-called critical interval of biomeres between the initial and final phases of extinction. There are no biostratigraphic data available for cores 1EE and 12EE.

SUPPLEMENTARY MATERIALS

REFERENCES AND NOTES

1. M. Foote, Origination and extinction through the Phanerozoic: A new approach. *J. Geol.* **111**, 125–148 (2003).
2. R. K. Bambach, A. H. Knoll, S. C. Wang, Origination, extinction, and mass depletions of marine diversity. *Paleobiology* **30**, 522–542 (2004).
3. B. C. Gill, T. W. Lyons, S. A. Young, L. R. Kump, A. H. Knoll, M. R. Saltzman, Geochemical evidence for widespread euxinia in the Later Cambrian ocean. *Nature* **469**, 80–83 (2011).
4. D. S. Jones, D. A. Fike, Dynamic sulfur and carbon cycling through the end-Ordovician extinction revealed by paired sulfate–pyrite δ^{34}S. *Earth Planet. Sci. Lett.* **363**, 144–155 (2013).
5. M. R. Saltzman, C. T. Edwards, J. M. Adrain, S. R. Westrop, Persistent oceanic anoxia and elevated extinction rates separate the Cambrian and Ordovician radiations. *Geology* **43**, 807–810 (2015).
6. M. Saltzman, E. Thomas, in *The Geologic Time Scale*, F. M. Gradstein, J. G. Ogg, M. Schmitz, G. Ogg, Eds. (Elsevier, 2012), pp. 207–232.
7. M. R. Saltzman, R. L. Ripperdan, M. Brasier, K. C. Lohmann, R. A. Robison, W. Chang, S. Peng, E. Ergaliev, B. Runnegar, A global carbon isotope excursion (SPICE) during the Late Cambrian: Relation to trilobite extinctions, organic-matter burial and sea level. *Palaeogeogr. Palaeoclimatol. Palaeoecol.* **162**, 211–223 (2000).
8. T. Servais, O. Lehnert, J. Li, G. L. Mullins, A. Munnecke, A. Nützel, M. Vecoli, The Ordovician biodiversification: Revolution in the oceanic trophic chain. *Lethaia* **41**, 99–109 (2008).
9. M. R. Saltzman, S. A. Young, L. R. Kump, B. C. Gill, T. W. Lyons, B. Runnegar, Pulse of atmospheric oxygen during the late Cambrian. *Proc. Natl. Acad. Sci. U.S.A.* **108**, 3876–3881 (2011).
10. T. W. Dahl, R. A. Boyle, D. E. Canfield, J. N. Connelly, B. C. Gill, T. M. Lenton, M. Bizzarro, Uranium isotopes distinguish two geochemically distinct stages during the later Cambrian SPICE event. *Earth Planet. Sci. Lett.* **401**, 313–326 (2014).
11. J. G. Metzger, D. A. Fike, Techniques for assessing spatial heterogeneity of carbonate δ^{13}C values: Implications for craton-wide isotope gradients. *Sedimentology* **60**, 1405–1431 (2013).

12. P. K. Swart, G. Eberli, The nature of the δ¹³C of periplatform sediments: Implications for stratigraphy and the global carbon cycle. *Sediment. Geol.* **175**, 115–129 (2005).

13. J. Palmer, T. L. Thompson, C. Seeger, J. F. Miller, J. M. Gregg, The Sauk megasequence from the Reelfoot Rift to southwestern Missouri. *AAPG Mem.* **93**, 1013–1030 (2012).

14. V. E. Kurtz, Franconian (Upper Cambrian) trilobite faunas from the Elvins Group of southeast Missouri. *J. Paleontol.* **49**, 1009–1043 (1975).

15. A. Palmer, Biomere boundaries re-examined. *Alcheringa* **3**, 33–41 (1979).

16. A. R. Palmer, The biomere problem: Evolution of an idea. *J. Paleontol.* **58**, 599–611 (1984).

17. J. H. Stitt, Repeating evolutionary pattern in Late Cambrian trilobite biomeres. *J. Paleontol.* **45**, 178–181 (1971).

18. J. Taylor, History and status of the biomere concept. *Mem. Assoc. Australas. Palaeontol.* **32**, 247 (2006).

19. J. H. Stitt, Adaptive radiation, trilobite paleoecology, and extinction, Ptychaspid Biomere, Late Cambrian of Oklahoma. *Fossils Strata* **4**, 381–390 (1975).

20. S. R. Westrop, Trilobite diversity patterns in an Upper Cambrian stage. *Paleobiology* **14**, 401–409 (1988).

21. S. R. Westrop, R. Ludvigsen, Biogeographic control of trilobite mass extinction at an Upper Cambrian "biomere" boundary. *Paleobiology* **13**, 84–99 (1987).

22. Z. He, J. M. Gregg, K. L. Shelton, J. R. Palmer, in *Basin-Wide Diagenetic Patterns: Integrated Petrologic, Geochemical, and Hydrologic Considerations*, I. P. Montañez, J. M. Gregg, K. L. Shelton, Eds. (Society for Sedimentary Geology, 1997), pp. 81–99.

23. S. Peng, L. Babcock, R. Robison, H. Lin, M. Rees, M. Saltzman, Global Standard Stratotype-section and Point (GSSP) of the Furongian Series and Paibian Stage (Cambrian). *Lethaia* **37**, 365–379 (2004).

24. V. E. Kurtz, J. L. Thacker, K. H. Anderson, P. E. Gerdemann, *Traverse in Late Cambrian Strata from the St. Francois Mountains, Missouri to Delaware County, Oklahoma* (Missouri Geological Survey, 1975).

25. M. R. Saltzman, C. A. Cowan, A. C. Runkel, B. Runnegar, M. C. Stewart, A. R. Palmer, The Late Cambrian Spice (δ¹³C) Event and the Sauk II-SAUK III regression: New evidence from Laurentian Basins in Utah, Iowa, and Newfoundland. *J. Sediment. Res.* **74**, 366–377 (2004).

26. A. M. Gerhardt, B. C. Gill, Elucidating the relationship between the later Cambrian end-Marjuman extinctions and SPICE Event. *Palaeogeogr. Palaeoclimatol. Palaeoecol.* **461**, 362–373 (2016).

27. C. Holmden, R. Creaser, K. Muehlenbachs, S. A. Leslie, S. M. Bergström, Isotopic evidence for geochemical decoupling between ancient epeiric seas and bordering oceans: Implications for secular curves. *Geology* **26**, 567–570 (1998).

28. D. S. Jones, D. A. Fike, S. Finnegan, W. W. Fischer, D. P. Schrag, D. McCay, Terminal Ordovician carbon isotope stratigraphy and glacioeustatic sea-level change across Anticosti Island (Québec, Canada). *Geol. Soc. Am. Bull.* **123**, 1645–1664 (2011).

29. A. Immenhauser, G. Della Porta, J. A. M. Kenter, J. R. Bahamonde, An alternative model for positive shifts in shallow-marine carbonate δ¹³C and δ¹⁸O. *Sedimentology* **50**, 953–959 (2003).

30. B. Dyer, A. C. Maloof, Physical and chemical stratigraphy suggest small or absent glacioeustatic variation during formation of the Paradox Basin cyclothems. *Earth Planet. Sci. Lett.* **419**, 63–70 (2015).

31. W. P. Patterson, L. M. Walter, Depletion of ¹³C in seawater ΣCO₂ on modern carbonate platforms: Significance for the carbon isotopic record of carbonates. *Geology* **22**, 885–888 (1994).

32. G. K. Ergaliev, in *Short Papers for the Second International Symposium on the Cambrian System* (U.S. Geological Survey, 1981), pp. 82–88.

33. S. Peng, R. A. Robison, Agnostoid biostratigraphy across the Middle–Upper Cambrian boundary in Hunan, China. *J. Paleontol.* **74**, 1–104 (2000).

34. P. M. Myrow, J. P. Grotzinger, Chemostratigraphic proxy records: Forward modeling the effects of unconformities, variable sediment accumulation rates, and sampling-interval bias, in *Carbonate Sedimentation Diagenesis Evolving Precambrian World* (Society for Sedimentary Geology, 2000), pp. 43–55.

35. P. J. Perfetta, K. L. Shelton, J. H. Stitt, Carbon isotope evidence for deep-water invasion at the Marjumiid-Pterocephaliid biomere boundary, Black Hills, USA: A common origin for biotic crises on Late Cambrian shelves. *Geology* **27**, 403–406 (1999).

36. J. H. Stitt, P. J. Perfetta, Trilobites, biostratigraphy, and lithostratigraphy of the *Crepicephalus* and *Aphelaspis* zones, lower Deadwood Formation (Marjuman and Steptoean stages, Upper Cambrian), Black Hills, South Dakota. *J. Paleontol.* **74**, 199–223 (2000).

37. M. T. Hurtgen, S. B. Pruss, A. H. Knoll, Evaluating the relationship between the carbon and sulfur cycles in the later Cambrian ocean: An example from the Port au Port Group, western Newfoundland, Canada. *Earth Planet. Sci. Lett.* **281**, 288–297 (2009).

38. B. C. Gill, T. W. Lyons, M. R. Saltzman, Parallel, high-resolution carbon and sulfur isotope records of the evolving Paleozoic marine sulfur reservoir. *Palaeogeogr. Palaeoclimatol. Palaeoecol.* **256**, 156–173 (2007).

39. B. Kendall, T. Komiya, T. W. Lyons, S. M. Bates, G. W. Gordon, S. J. Romaniello, G. Jiang, R. A. Creaser, S. Xiao, K. McFadden, Y. Sawakij, M. Tahatak, D. Shul, J. Hanl, Y. Lim, X. Chun, A. D. Anbarb, Uranium and molybdenum isotope evidence for an episode of widespread ocean oxygenation during the late Ediacaran Period. *Geochim. Cosmochim. Acta* **156**, 173–193 (2015).

40. E. L. Rowan, D. L. Leach, Constraints from fluid inclusions on sulfide precipitation mechanisms and ore fluid migration in the Viburnum Trend lead district, Missouri. *Econ. Geol.* **84**, 1948–1965 (1989).

41. J. Viets, E. Mosier, M. Erickson, in *International Conference of Mississippi Valley-Type Lead Zinc Deposits* (University of Missouri-Rolla, 1983), pp. 174–186.

42. D. F. Sibley, J. M. Gregg, Classification of dolomite rock textures. *J. Sediment. Res.* **57**, 968 (1987).

43. S. Peng, L. E. Babcock, R. A. Cooper, in *The Geologic Time Scale*, F. M. Gradstein, J. G. Ogg, M. Schmitz, G. Ogg, Eds. (Elsevier, 2012), pp. 437–488.

44. S. Peng, L. E. Babcock, J. Zuo, X. Zhu, H. Lin, X. Yang, Y. Qi, G. Bagnoli, L. Wang, Global Standard Stratotype-Section and Point (GSSP) for the base of the Jiangshanian Stage (Cambrian: Furongian) at Duibian, Jiangshan, Zhejiang, Southeast China. *Episodes* **35**, 462–477 (2012).

45. J. F. Taylor, J. E. Repetski, J. D. Loch, S. A. Leslie, Biostratigraphy and chronostratigraphy of the great American carbonate bank. *AAPG Mem.* **98**, 15–35 (2012).

46. J. Miller, Conodonts as biostratigraphic tools for redefinition and correlation of the Cambrian–Ordovician boundary. *Geol. Mag.* **125**, 349–362 (1988).

Citation: J. D. Schiffbauer, J. W. Huntley, D. A. Fike, M. J. Jeffrey, J. M. Gregg, K. L. Shelton, Decoupling biogeochemical records, extinction, and environmental change during the Cambrian SPICE event. *Sci. Adv.* **3**, e1602158 (2017).